A Reusable Solar-Electric Orbit Transfer Service

C. Colin Helms,[1] and Don V. Black, Ph.D.[2]
American Institute for Research in Science and Technology, Sheridan, Wyoming, 82801, USA

This report describes a commercial service for geosynchronous orbit transfer that is composed of a reusable solar-electric orbit transfer vehicle and infrastructure to store and transfer propellant on-orbit. The service is characterized as being able to transport 4-12 metric ton payloads to orbits in cis-Lunar space, specifically geosynchronous orbit. The service includes an orbit transfer vehicle composed of commercially available Hall-effect thrusters and solar arrays. The vehicle is sized to achieve a mission rate that provides a theoretical operating profit for a business. As the required power is on the scale of hundreds of kilowatts, an on-orbit assembly sequence is proposed to assemble such a vehicle. A scheme for in-orbit propellant resupply is introduced, centered around the approach of tank replacement and leveraging high performance launch vehicles to spread costs of propellant launch over several missions. The orbit transfer mission is assessed with trajectory analysis using an Edelbaum-Alfano control law. The analysis trades off required propellant mass and time of flight for several classes of vehicles optimized for power-plant mass and payload. Trajectories are simulated in four different eclipse seasons for year 2020 and the impact of eclipse on the mission is assessed. Payload mass up to 20 metric tons is also considered. The service improves on standard geosynchronous transfer orbits by delivering payload direct to geosynchronous inclination, which provides benefit to the payload client. The claim is made that the low mass requirement using electric propulsion and long-term storability of its propellants enables the service to be developed and operated commercially with resupply of propellant from Earth.

Nomenclature

AOP = Argument of Perigee
AOL = Argument of Latitude
ECA = Extended Capability Adapter
EML1 = Earth-Moon L1
EMD = Engineering Manufacturing and Development
ETR = Eastern Test Range
EOTV = Electric Orbit Transfer Vehicle
GTO = Geosynchronous Transfer Orbit
GEO = Geosynchronous Equatorial Orbit
GMAT = General Mission Analysis Tool
GSAT = Geosynchronous Satellite
GSLV = Geosynchronous Satellite Launch Vehicle
HET = Hall-Effect Thruster
η = Power efficiency of the propulsion system
I_{sp} = Specific Impulse
ILS = International Launch Services
ISRO = Indian Space Research Organization
ISRU = In-Situ Resource Utilization
ISS = International Space Station
JGM = Joint Earth Gravity Model

[1] Consultant, Freelance Rocket Science, AIAA Senior Member.
[2] President, American Institute for Research in Science and Technology, AIAA Member.

LAM = Liquid Apogee Motor
LEO = Low Earth Orbit
LH2 = Liquid Hydrogen
LOX = Liquid Oxygen
L1 = Lagrangian Point 1
MT = Metric Tons (1000-kilograms)
m_0 = Initial mass of orbit transfer vehicle
m_w = Mass of power plant
m_s = Mass of structure
m_p = Mass of propellant
m_{pl} = Mass of payload
m_{bo} = Mass of vehicle and payload at fuel depletion
N = Newtons (kg-m/s^2)
NRE = Non-Recurring Engineering
OTV = Orbit Transfer Vehicle
PL = Payload
PMK = Propellant Mission Kit
RAAN = Right Ascension of Ascending Node
RASC = Revolutionary Aerospace Systems Concepts (NASA 2012 study)
RPO = Rendezvous and Proximity Operations
SAFT = *La Societe Industrielle des Accumulateurs Alcans*, corporate name
SEP = Solar-Electric Propulsion
SMA = Semi-Major Axis
SMAD = Space Mission Analysis and Design, book title
SRP = Solar Radiation Pressure
TA = True Anomaly
TRL = Technology Readiness Level
UTJ = Ultra Triple Junction (Solar Cells)
USD = United States Dollars
XTJ = Next generation Triple Junction (Solar Cells)
ULA = United Launch Alliance, corporate name
VNB = Velocity Normal Binormal
WTR = Western Test Range

I. Introduction

There is a profound economic need to bring down the cost of access to space. With international competition, and the advent of reusable two-stage to orbit boosters, worldwide launch services are making inroads on the costs of launch. However, the basic chemistry of rocket propellants places a ceiling on the economics that can be achieved by this technology. Boosters such as the Falcon Heavy provide impressive payload mass capability, but no satisfactory solution for reusability of the upper stage has emerged. Furthermore, the large propellant mass required to achieve the altitude and inclination of a geosynchronous orbit limits the capability of even these high performing two-stage rockets. When payload mass exceeds 4000-kg, these vehicles offer only an elliptical transfer orbit which terminates short of equatorial inclination. The two-fold constraint on lowering the cost of access to space is propellant mass and upper stage reusability.

Reusability brings into play a fixed cost; the price for launch of the propellant for the mission and return of the vehicle. It is this cost that renders a reusable chemical Orbit Transfer Vehicle non-economic. It is more economical to perform a single launch with an expendable OTV and payload with the one-way required mass of fuel.

The higher specific impulse of an electrically propelled orbit transfer vehicle leads to a lower total mass of propellant, for both transfer and return. This difference in fuel mass should provide the margin that enables such a service to be profitable.

This report seeks to support that thesis using thrusters and power plants that are currently available in the marketplace, loosely referred to as “off-the-shelf.”

It is an attractive alternative to refuel a chemical upper stage via a cryogenic propellant depot. Kutter [1] performed a commercially based analysis of such a solution using propellant resupply from a propellant depot located at the Earth-Moon Lagrangian point 1 (EML1). His analysis leveraged reuse of the ULA Advanced Cryogenic Evolved

Stage, which is conceived with a pre-planned improvement for a propellant transfer interface. Kutter identifies an economic break-even point of $5M per ton of propellant for reusability, which is not achievable with launch of LH2/LOX from Earth. He proposes Lunar In-Situ Resource Utilization (ISRU) as the solution; mining oxygen and hydrogen from Lunar water.

Other analysts and teams have studied the problem, Thomas Perrin [2] provides an in-depth trade study for each orbital option in the architecture of such a depot.

One of the technology problems to be solved is long term storage of cryogenic propellants in orbit [2]. Cryogenic propellants are subject to challenges associated with controlling the phase change and boil-off of these propellants. Fikes, et al [3] note that though cryogenic fluid management has been analyzed extensively, there is remarkably little flight data to validate the analysis. At an estimated TRL4, these technologies are at best 10-15 years away from operational use.

We propose a near-term solution for reusable orbit transfer based upon the storability of electric propellants; xenon, or iodine, and the moderately high specific impulse of Hall-Effect Thrusters. We focus our analysis on geosynchronous orbit transfer since current launch services and their costs are well characterized and because it is remarkably costly to achieve geosynchronous equatorial orbit (GEO). The delta-V and number of maneuvers required to achieve Lunar orbit vs. GEO are comparable.

If the geosynchronous service can be economically operated, the same service has the capability to transfer sizeable cargo to high Lunar orbit, and other useful orbits such as Earth-Moon L1 halo orbits. The capability to economically transport large payloads to destinations in cis-Lunar space should provide a necessary stepping-stone in the development of future in-orbit infrastructure, such as the Deep-Space Gateway, Lunar ISRU architectures, and the In-Space Cryogenic Propellant Depot.

II. The Geosynchronous Launch Market

A reusable orbit transfer service can be characterized as an extension of the current LEO launch services, a replacement for the chemical upper stage rather than a replacement for the entire launch service. To characterize the state of current geosynchronous orbit services, it is instructive to examine these services' payloads, costs and capabilities.

Payloads are rarely delivered directly into an equatorial inclination at geosynchronous altitude. This mission simply requires too much propellant to both execute the inclination change and achieve altitude. Instead, launch services provide a Geosynchronous Transfer Orbit (GTO).

Figure 1 shows that 68% of the launches to GTO in period of March 2016 to March 2018 were payloads between 4 and 12 metric tons.

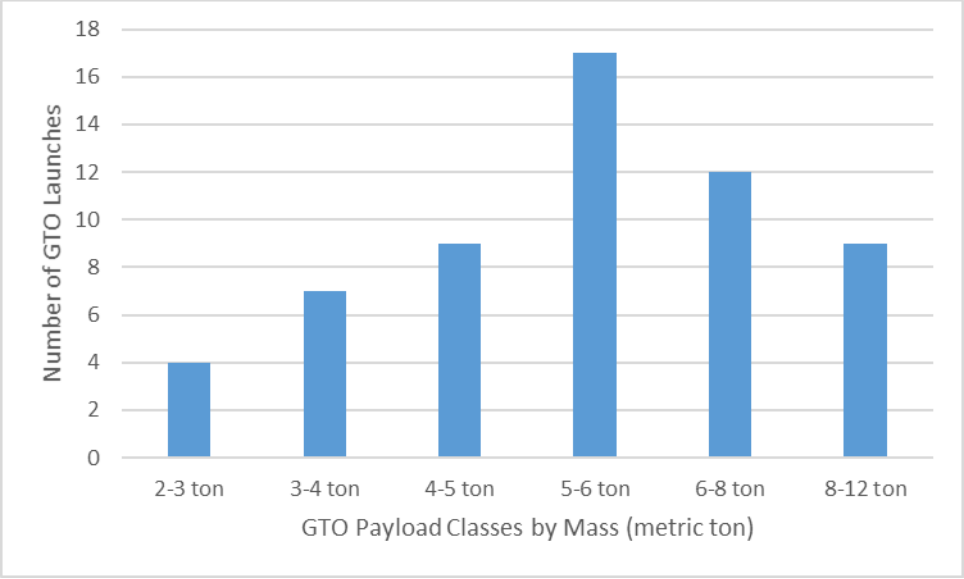

Figure 1, Distribution of Launches by Payload Mass

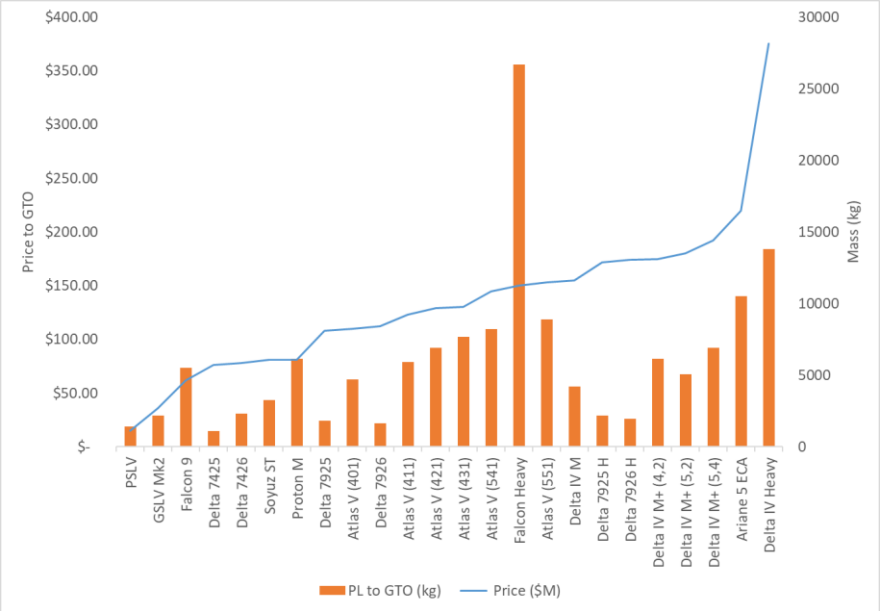

Figure 2, Capability vs "Flyaway" Price for GTO Launch

Figure 2 shows capability and price for various GTO launch services, where the blue scatter line represents the price per launch[3] and the histogram represents the mass capability of each launch vehicle. The mass of the payload capability is shown at the right axis. Falcon Heavy represents the outlier in capability at the center of the chart.

Figure 2 indicates the least expensive cost of launch into GTO for a 4-ton payload is Falcon 9, with a price of $61M. Next is Proton at $82M, and then Falcon Heavy with a pre-production price range from $98M to $150M. SpaceX has demonstrated in the greater than 33 successful Falcon 9 launches that it is a disruptive force in the GTO market, the other launch providers are being forced to rapidly improve their economics or go out of business.

The service we consider here includes the starting requirement that the service shall transfer client payloads direct to equatorial orbit. Ariane 5 publishes a price of $220M for a similar service, enabled by its launch site at Kourou on the equator. Arianespace manages these launch manifests and the Extended Capability Adapter (ECA) version of Ariane 5 is capable of manifesting two payloads [4]. Arianespace is mute on the capability of the ECA version, but the launch of Sky Muster-2 co-manifested with GSAT-18 on 5 October 2016 reveals that Ariane 5 ECA can launch up to a 10-ton aggregate payload mass into a 3-degree inclination GTO [5].

By comparison with Ariane 5 and given Figure 1, we derive two additional requirements for the reusable orbit transfer service. The service shall manifest multiple payloads and the service shall transfer an aggregate payload mass of up to 12 metric tons.

III. Incompleteness of Geosynchronous Launch Services

When an Orbit Transfer Vehicle (OTV) can deliver a satellite payload directly into equatorial inclination at geosynchronous altitude, the satellite payload no longer needs to carry excess propellant for the orbit transfer in its mass budget. The result is that its revenue or utility and useful life of the satellite is improved. Only the largest classes of launch vehicle, or vehicles which launch from sites near the equatorial latitude, have the capability to perform this service.

Given the latitude of a launch site, launch geometry enforces a floor on the inclination the service can reach, for instance a due East launch from a latitude provides the lowest inclination that can be reached in a direct launch. Since an inclination change is the most expensive maneuver in terms of propellant, launch services typically leave a great deal of residual inclination and circularization delta-V at payload separation.

[3] The prices shown in Figure 2 are “flyaway” prices gleaned from a number of public sources [25] [29] [27] [23]. “Flyaway” prices are manufacturer’s prices and do not include options such as delivery to any orbit, mission analysis, payload separation system, launch site telemetry, environmental monitoring, etc.

The result is that in a standard Geosynchronous Transfer Orbit (GTO) the payload is released into an orbit that is highly elliptical and inclined. For instance, the Atlas V User's Guide, launching from the Eastern Test Range (ETR) at latitude 28.5-degrees defines its standard GTO as 185-km by 35786-km inclined at 27 degrees [6]. The client satellite must make-up some 1800 m/s of delta-v using this GTO service.

As a specific example of a GTO, the GSAT-6A spacecraft was launched by the Indian Space Research Organization (ISRO) on their Mark 2 Geosynchronous Satellite Launch Vehicle (GSLV Mk.2) 29 March 2018 [7]. We performed a simulation of this GTO mission using the NASA General Mission Analysis Tool (GMAT) [8]. Figure 3 shows the results of the simulation.

The simulation uses a satellite launch mass of 2140-kg, and a Liquid Apogee Motor with a specific impulse of 269-sec [9]. The GSAT-6A[4], starting orbit is 149-km by 36,508-km with a 20.7-degree inclination. This initial orbit required the GSAT-6A Liquid Apogee Motor (LAM) to perform a 20.5-degree inclination change, a drift to orbit at 83-degrees E longitude and a final circularization burn [10]. The GMAT report file gives the delta-V required for this chain of maneuvers as 2403m/s and a calculation gives the propellant fuel mass as 1280-kg. We characterize this fuel as the mass penalty for this particular satellite.

The dollar value of the mass penalty provides insight into the value a direct to GEO mission may provide. A C/Ku-band commercial satellite with a 280-kg payload will provide 24-48, 36MHz-wide transponders. Based on a market price average of $2000 USD per month per MHz, each additional transponder represents a potential monthly revenue of $28,800 USD. Conservatively assuming 40% of capacity is sold on average over the 15-year satellite life, and 3% inflation, the Future Value of 24 additional transponders is $4.689B, with a current year value of $313M USD. Given the client is a standard geosynchronous communications satellite, the client receives a benefit of $313M in the first year of additional capacity, enabled by a direct to equatorial inclination orbit transfer service.

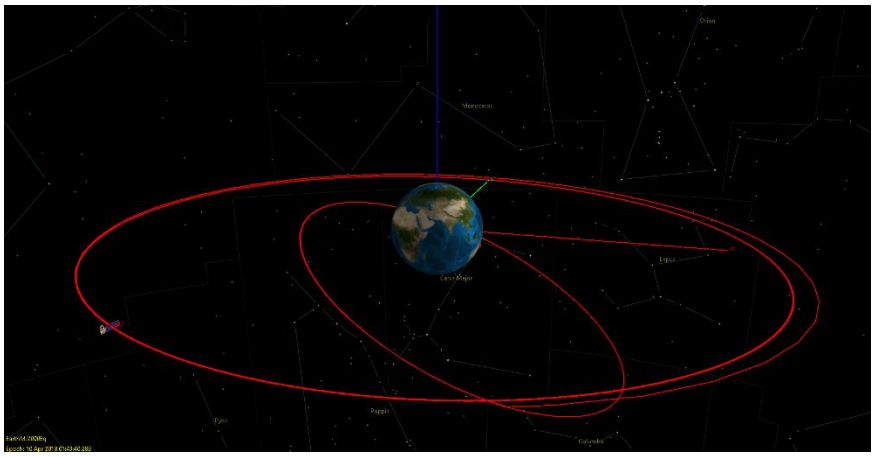

Figure 3, GSAT-6A GTO Mission

IV. Mission Analysis

The mission objectives for the reusable orbit transfer service are listed in Table 1.

Table 1, Top Level Mission Objectives and Constraints

Rank	Top Level Objective	Constraints
Primary	P.1. Transfer 4 – 12-ton payload mass to low inclination geo-synchronous orbit.	C.1. Operating Profit > $600M per year
Secondary	S.1. Provide service to customers from disadvantaged launch latitudes.	C.2. Circular LEO rendezvous orbit
	S.2. Provide the service in the mid 2020's.	C.3. Use components with TRL-5 or above

[4] GSAT-6A suffered a power failure during the circularization burn.

Objective (S.1) states the mission is to transfer large payloads (4 – 12-metric ton range) to geosynchronous orbit. This mission will require thrust in the range of 5 – 30 newtons assuming a low-thrust, solar-electric vehicle.

Constraint (C.1) is intended to make such a service commercially realizable. The $600M figure is comparable to, but below the Lockheed Martin Corporation report of $993M operating profit for its space sector in its 2017 4th quarter Consolidated Statement of Earnings [11].

Constraint (C.2) is necessary to be able to take delivery of client payloads in-orbit, as well as resupply propellant. Rendezvous and Proximity Operations (RPO) are necessary and have only been successfully demonstrated in circular LEO orbit to date.

Objectives (S.1), (S.2) and Constraint (C.3) are discussed below.

Mass Considerations

For such a vehicle, the mission analysis must necessarily balance the payload mass to orbit vehicle mass. If an on-orbit assembly program is executed, the structural mass fraction for the zero-g vehicle will be small compared to the power plant mass. The vehicle initial mass in LEO, $m_{0,}$ is primarily propellant and power plant.

In 1962, Melbourne and Sauer presented a thorough analysis of the optimization of the payload for propulsion system and payload mass in power limited vehicles with coast periods [12]. They formulated the Hamiltonian with adjoint constraints on payload and power supply mass and derived several findings.

They note that an on-orbit assembly sequence allows the structural mass to be neglected in the optimization, focusing on the power supply, payload and propellant mass.

For any electric thruster the following relationship holds,

$$T/P = 2\eta/I_{sp} g_0 \tag{1}$$

Where:

- η = Power efficiency of the propulsion system
- I_{sp} = specific impulse
- g_0 = 9.81-m/s^2
- P = Propulsion input power
- T = Thrust

As a condition for maximizing payload, the following relationship between efficiency and specific impulse is asserted by Melbourne and Sauer as a theorem,

$$I_{sp} \frac{1}{\eta} \frac{\partial \eta}{\partial I_{sp}} < 1 \tag{2}$$

This condition results in the simultaneous minimization of thrust and mass-flow rate for given power supply mass ratio and specific power. Practically, it indicates that the thruster should operate so that the variation in efficiency with I_{sp} is as small as possible.

Melbourne and Sauer provides an approximation formula for optimum power supply mass for use in mission analysis. We provide details in Appendix A.

Eq. (1) shows that thruster efficiency varies with input power and thrust. For a given specific impulse, a constant thrust vehicle should hold beam-voltage as constant as possible. This assertion prefers a solution with regulated voltage from the solar arrays.

Comparison to Prior Studies

A study of a Solar-Electric Propulsion (SEP) mission was performed by Thomas Kerslake and Leon Gefert in 1999 for transfer of an 80-ton cargo to an 800 x 65000-km parking orbit [13]. The SEP vehicle was conceived with a 35-ton dry mass, 5800 m^2 of solar array area and eight 100 kW Hall-Effect thrusters with specific impulse in the range 2000-3000s. Their vehicle concept has aggregate thrust of 6N.

Another trade-off between Hall-Effect and gridded ion electric propulsion was performed in NASA's Revolutionary Aerospace Systems Concepts (RASC) study. The RASC objective was to transfer 36-ton payloads from LEO to EML1 [14]. The authors selected gridded ion thrusters in this study with rationale that they have lower

total propellant requirements for the mission. The resultant vehicle has a dry mass of 11.3-tons, uses eight thrusters, each with input power 49.5 kW, *Isp* of 3300-sec and life of 15,000 hours; the maximum thrust available from this configuration is 20N.

Both of the above studies rely on development of technology; high voltage power management, advanced thrusters and solar array configurations. The work herein focuses on a vehicle which is realizable within the next 10 years. That tenet requires that we forego advanced power and thruster concepts with preference for equipment and components that are TRL-5 as a minimum and better, are in use on-orbit currently (TRL-9).

The power source selected for this vehicle uses deployable Solar Array panels which are commercially available. The technology has been flown in geosynchronous satellite configurations exceeding 25 kW [15]. We have notionally set the vehicle main bus voltage to 160VDC, the highest voltage for which space qualified power management systems and solar array circuits are known to be available. For example, this main bus voltage is distributed on the ISS [16].

We considered only thruster technology which is catalog ready from companies including Aerojet, Safran, and Busek. The Busek company produces an 8-kW Hall-Effect thruster with *Isp* in the range of 1900 – 2200s and efficiencies of 55 to 65%. Table 2 identifies a subset of the reported throttle characteristics for the Busek BHT-8000, selected for close values of efficiency [17].

Life is an important selection criterion for a reusable OTV. The magnetic field for this thruster, the BHT-8000, is designed to achieve a condition of zero channel erosion, its projected life time is >50,000 hours [17]. The projected life of these thrusters at 55% duty cycle exceeds 10 years of on-orbit life.

Table 2, BHT-8000 Reported Characteristics, IEPC-13-317

Voltage	Power	Thrust (N)	Isp	Efficiency
350	4063	0.245	1927	0.56
350	5999	0.365	1977	0.57
350	8060	0.465	1979	0.57

Correspondence with the Busek company indicates that the tested performance of the BHT-8000 thruster is somewhat better than reported in 2013 and is shown in Table 3 [18].

Table 3, BHT-8000 Tested Characteristics

Voltage	Power	Thrust (N)	Isp	Efficiency
400	4537	0.260	2077	0.58
400	6295	0.359	2165	0.61
400	8061	0.449	2217	0.61

Vehicle Configurations

The key performance parameters of the trade study for the OTV are propellant mass and time of flight. Propellant mass will deeply impact the fixed costs of the service. Time of flight will impact the rate at which revenue can be earned. Mass is determined from a mass model which is described in Appendix B.

We use the approximation criteria of Melbourne and Sauer to identify the optimum vehicle configurations for the desired payload range from multiple proposed configurations of HETs operating at various power settings. A vehicle configuration of 32 Hall-Effect Thrusters operating at the 8061W power level provides optimal performance for 8-12-ton payloads. Details are provided in Appendix A and characteristics of the selected vehicle configurations are shown in Table 4.

Given that NASA is interested in payload mass up to 36-tons to EML1 [14], we also carry out the optimization for the 64x6295W and 64x8061W configurations. We find that the 64x8061 vehicle configuration is optimum for 24-36-ton payloads.

Vehicle configurations that are indicated as optimum for 4-ton payloads are not further analyzed since the 4-ton payload does not support a multiple manifest.

Mission Analysis.

Objective S.1 in Table 1, Top Level Mission Objectives and Constraints, states, “Provide service to customers from disadvantaged launch latitudes.” This objective requires analysis of two cases for each vehicle configuration; one for 51.2-degree inclination and one for 28.5-degree inclination. Notwithstanding that the International Space

Station orbits at a 51.6-degree inclination, we selected 51.2 as the high inclination since it is reachable from Jiuquan, Baikonur, Satish Dhawan, Wallops Island, and Tanegashima launch sites [19].

We perform trajectory analysis using the NASA General Mission Analysis Tool (GMAT) to assess performance in the selected vehicle configurations per Table 4. The trajectory analysis is performed with the thruster parameters of Table 3, BHT-8000 Tested Characteristics.

Table 4, Vehicle Configurations found to be Optimal

Configuration	Payload Mass (kg)	Power (kW)	Total Thrust (N)	Alpha (kg/kW)	Initial Mass (kg)	Final Mass (kg)
32 HET, 8061W	8000	262.92	14.268	22	25138	16854
	12,000	262.92		22	30609	20854
64 HET, 6295W	16,000	388.94	22.976	27	48178	32256
	24,000	388.94		27	59119	40256
64 HET, 8061W	24,000	520.84	28.736	30	67350	45018
	36,000	520.84		30	83762	57018

Trajectory analysis is performed for the configurations of Table 4 using the Edelbaum-Alfano control law for combined inclination and orbit raising [20]. Our methods for computing the Edelbaum-Alfano trajectory are documented in Appendix C.

The spacecraft coordinate system used in this study is the Velocity-Normal-Binormal (VNB) coordinate system. In this system the $\hat{V}$ unit vector is defined parallel to the vehicle orbital velocity, the $\hat{N}$ unit vector is then normal to $\hat{V}$ and directed out of the orbit plane. The $\hat{B}$ unit vector is defined as parallel to the cross-product of $\hat{V}$ and $\hat{N}$. GMAT uses the VNB coordinate system by default.

It is important to understand the meaning of the term "yaw" in this system. There is much confusion in the writings on this subject with the original Edelbaum paper using the term "pitch". Aircraft and spacecraft define roll-pitch-yaw differently since for a spacecraft "the ground" is the orbital plane. We define vehicle yaw as a vector in the $\widehat{V \cdot N}$ plane, it is the out-of-plane thrust component.

Given this definition the Edelbaum-Alfano control law can be stated,

$$\vartheta(v) = \tan^{-1} \frac{\cos v}{\sqrt{{}^{1}/_{u(R)} - 1}} \tag{3}$$

Where:

$\vartheta(v)$, the yaw angle for an orbit ratio
v, the Argument of Latitude modulates the yaw angle
R, the current orbit ratio
u, trajectory scale factor, a function of R

We were initially concerned regarding the impact of eclipse on the orbital elements and surveyed adjustments to the trajectory following the methods of Kechichian [21] and Kluever [22].

Kechichian's method requires the simulation to update the Argument of Perigee upon each exit from earth shadow. We found this method to conflict with the Edelbaum-Alfano control law, as the cosine argument in the control law must be referenced to the nodes, which is the common intersection between planes.

The Kluever method [22] provides an approximation that is a simple computation of thrust weights as a function of sun angle. We found this is easily implemented using the GMAT thrust scale factor. Ultimately, we rejected the algorithm as it is uncertain how the variation in thrust magnitude in the simulation can be transferred to the constant thrust HET device.

During this study our data shows that the Edelbaum-Alfano control law is robust in the presence of eclipse. With no adjustment for eclipse whatsoever, the vehicle tends to arrive at geosynchronous altitude and equatorial inclination reliably with little error; 0.04-degrees inclination is typical. The main impact of eclipse is to time of flight and battery depth of discharge.

Figure 4 provides four example plots from the trajectory simulation. These are for the case of a transfer from 51.2 degrees inclination. Note that most of the inclination change is made at the large altitudes, which is indicative of an optimum plane change.

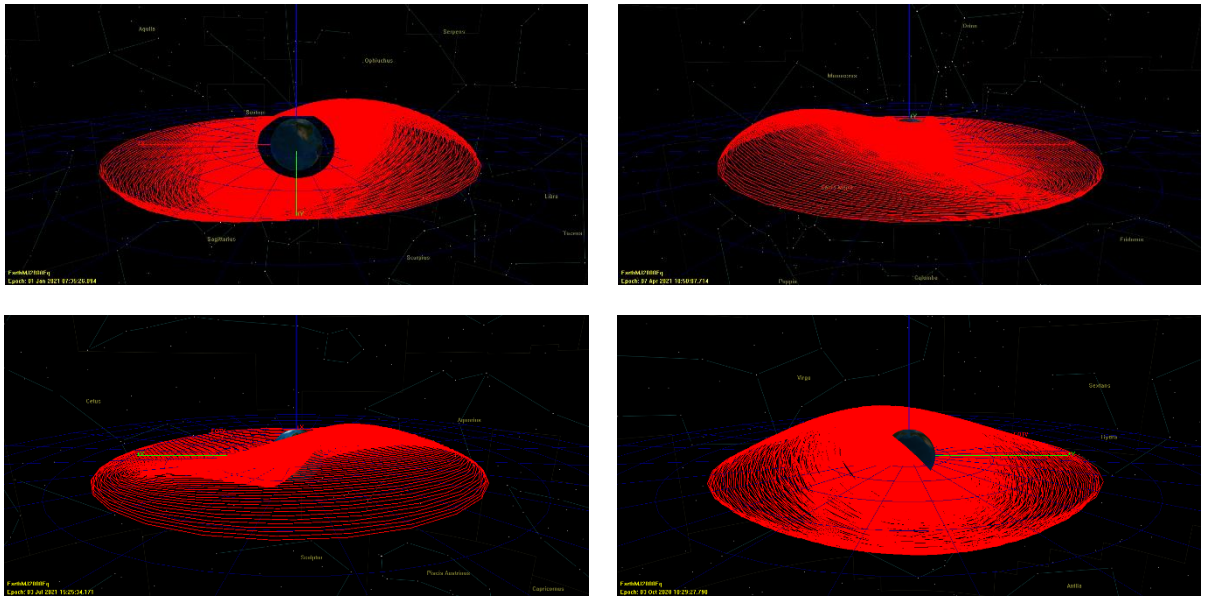

Figure 4, Alfano Transfers from 51.2-deg Inclination

Figure 5 shows the fuel consumption and flight duration of the 8-ton payload transfer from both 51.2-degree and 28.5-degree inclination. Performance for the 32-HET vehicle configuration using the 8061W throttle setting is shown in each of the four eclipse seasons.

Mission simulations were performed for Vernal Equinox, Summer Solstice, Autumnal Equinox, Winter Solstice. It is notable that there is little variation in mission duration or propellant usage due to the season of launch. We attribute this to averaging of the eclipse effect over 400 – 1200 revolutions over many days but the lack of variation was unexpected and deserves further investigation. One additional observation is that during winter and summer seasons missions the trajectory tended to "overshoot" the geosynchronous altitude, arriving with up to 0.5-degree of error in inclination. We compensate for this effect in the control law as discussed in Appendix C.

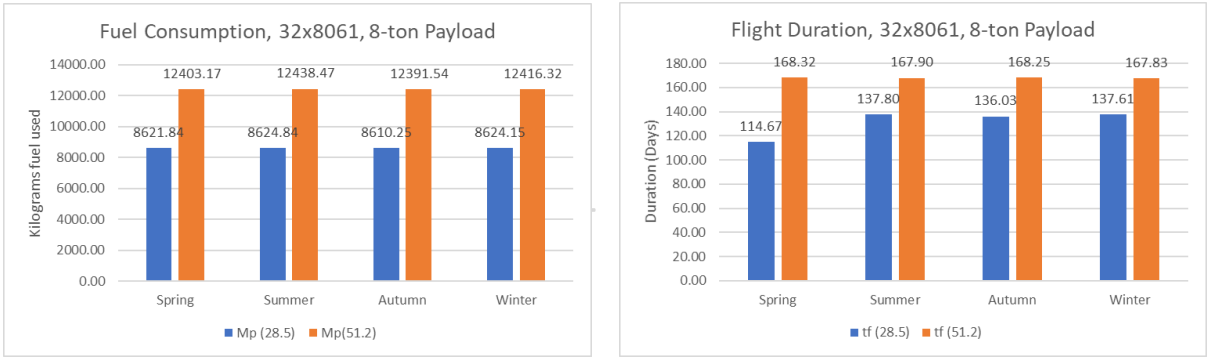

Figure 5, 32x8061 Vehicle Performance for 8-ton Payload

Figure 6 shows the fraction of propellant that must be reserved for the return flight. This mass is added to the transfer fuel requirement for each class of vehicle, and the trajectory is iterated to converge to a total propellant budget. The sum of the mission required mass and the return propellant mass is reflected in Figure 5.

The payload is separated at the geosynchronous destination, return time-of-flight and propellant usage is therefore independent of the payload size. The return flight duration ranges from 54 – 58 days to 28.5-deg inclination LEO and from 70 – 72 days to 51.2-deg inclination LEO in this configuration.

Figure 6, Fuel Reserve for 32x8061 Vehicle Return to LEO

Figure 7 shows the fuel consumption and flight duration of the mission for a 12-ton payload transfer using the 32-HET configuration at 8061W throttle setting. As above, performance is shown in each of the four eclipse seasons.

Return flight propellant usage is the same as shown in Figure 6.

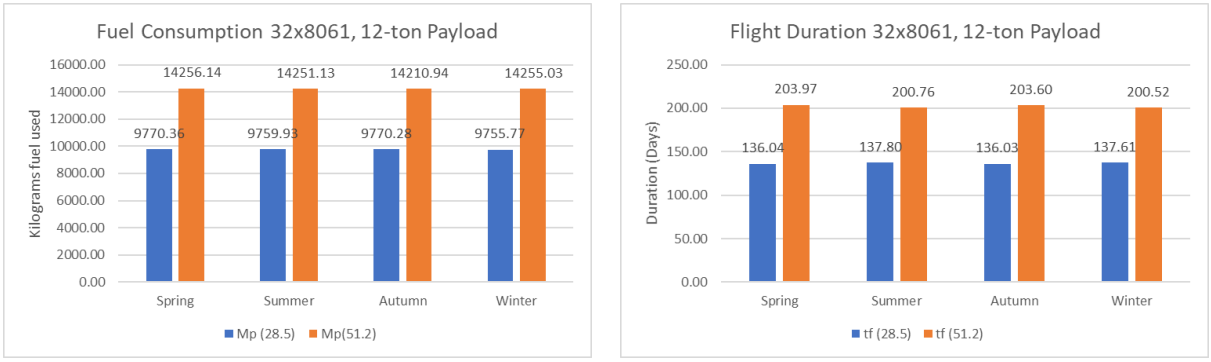

Figure 7, 32x8061 Vehicle Performance for 12-ton Payload

The trade-space for these options includes not only the time of flight and propellant required, but also the utility of a multi-payload manifest. The 32x8061 vehicle configuration is attractive since 8-12-ton payload transfers are optimum with its estimated thrust and mass. The question of whether this class of vehicle may close a business case is addressed below.

Melbourne and Sauer criteria indicate that the 64x6295 vehicle configuration is optimal for 16-24-ton payload transfer and the 64x8061 configuration is optimal for 24-36-ton payload transfers. The 36-ton payload is the objective mass to transfer to EML1 in the NASA RASC study [14].

Configurations with capacity up to 36 tons represent potential growth for the business. Given a trajectory solution for the constant, low-thrust vehicle to rendezvous with an EML1 halo orbit, vehicles of this size may provide logistics flights supporting the proposed cis-Lunar Gateway.

Figure 8, Figure 9 and Figure 10 show the performance for the 24-ton and 36-ton payloads in transfers to geosynchronous orbit using these configurations.

Figure 8 and Figure 9 represent a comparison of two different configurations for which the 24-ton payload is optimal. The 64x6295 configuration provides better fuel performance to geosynchronous orbit. The 64x8061 configuration provides better time of flight.

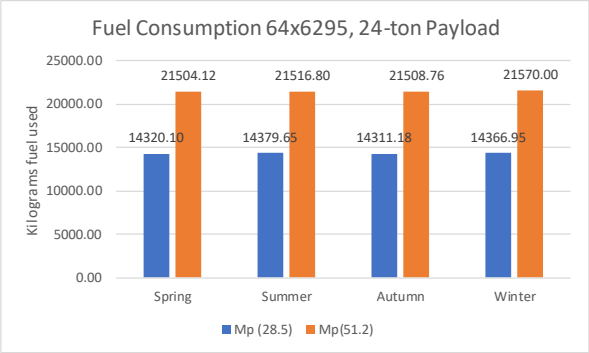

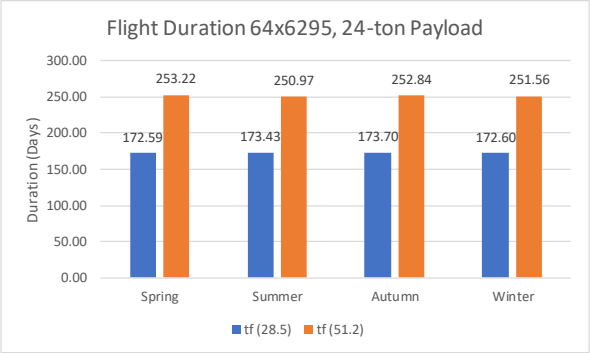

Figure 8, 64x6295 Vehicle Performance for 24-ton Payload

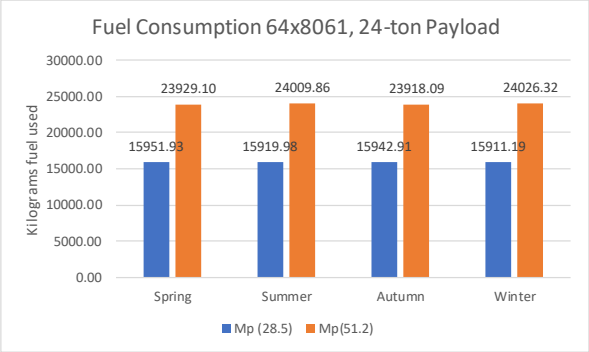

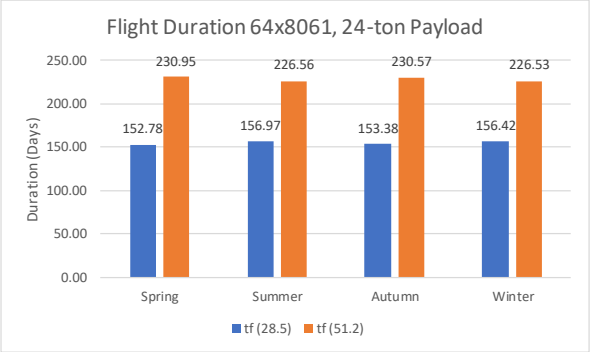

Figure 9, 64x8061 Vehicle Performance for 24-ton Payload

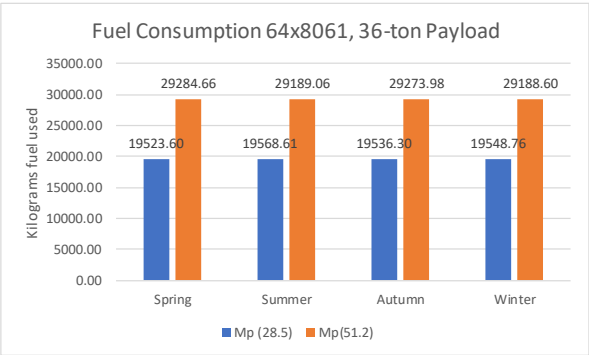

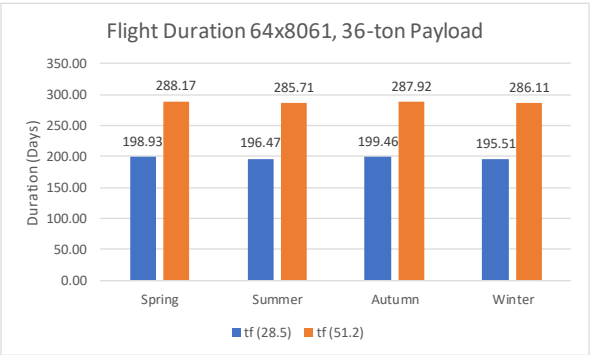

Figure 10, 64x8061 Vehicle Performance for 36-ton Payload

V. Concept of Operations

Figure 11 depicts the major elements envisioned for the reusable orbit transfer service. The 32x8061 configuration is realized in a notional vehicle shown in the lower half of the figure.

One of the features envisioned is on-orbit modularity. Modularity is necessary, the vehicle on this scale cannot be placed in orbit with a single launch. Restricted launch vehicle fairing volume and payload capacity drive the need for modularity and on-orbit assembly. Modularity also supports repair and replenishment of the vehicle.

The vehicle structure is constructed from trusses made of carbon composite tubing manufactured in standard sizes. Each member is designed to be mated structurally and electrically to its neighbor. The vehicle is configured with 8 propulsion modules, each supporting 4 Hall-Effect thrusters.

Thermal management is distributed across the functional modules. The power electronics module, battery module and propulsion module each are equipped with independent sets of passive thermal radiators. Each module is an Orbit Replacement Unit.

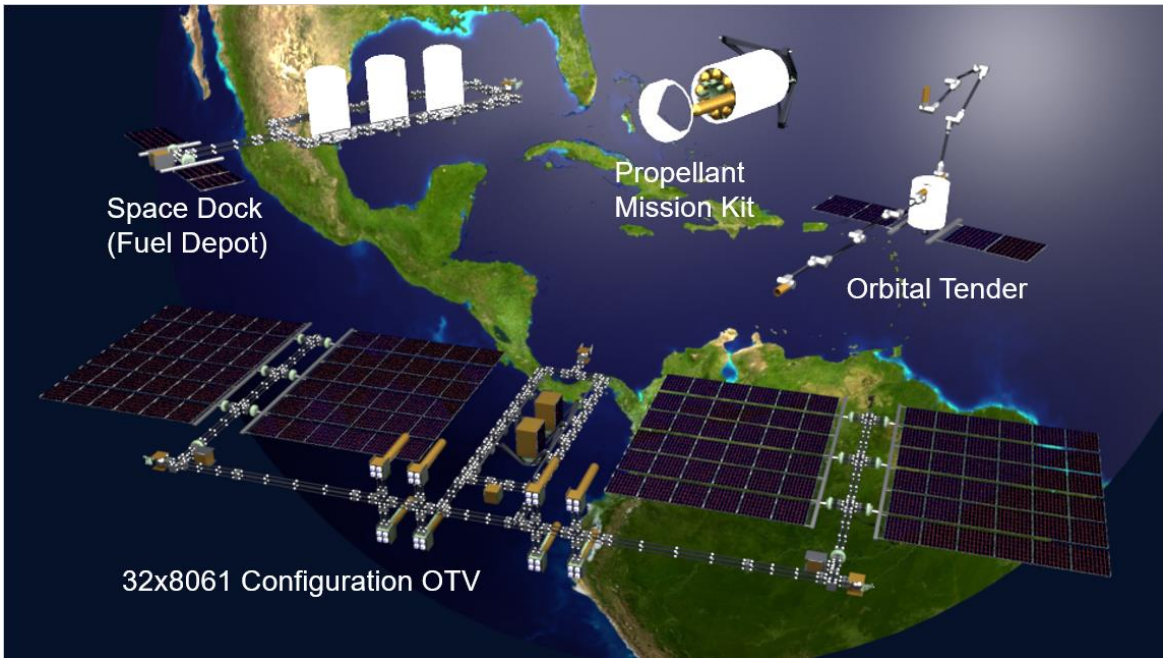

Figure 11, Reusable Orbit Transfer Operational View

Figure 11 bottom shows the OTV uses eight propulsion modules with four 8-kW Thrusters each. These are shown along the aft beam and include replaceable propellant tanks. The OTV payload bay is located amidships for weight and balance. It is envisioned with the 4.6 x 18.3-dimensions of the Space Shuttle payload bay and can transport up to 4 payloads mounted on cradles. Each cradle implements a payload separation interface.

A free-flying Propellant Mission Kit (PMK) is shown at upper center with one canister partially deployed. The PMK is provisioned earth-side and launched using an expendable booster.

The Space Dock at upper left is the propellant depot, shown with 3 berthed PMKs.

The Orbital Tender at upper right operates in LEO and is shown equipped with two robotic arms. The Tender is envisioned to maneuver using a simple monopropellant propulsion system. It performs Rendezvous and Proximity Operations (RPO) and berths to the Space Dock and OTV via an arm end-effector and grapple fixture. The key function of the Tender is to capture client payloads and PMKs from inertial orbit and berth them to the OTV or Space Dock.

VI. Conclusion

Architecture starts with a concept of operations, and the concept laid out above is quite large in scope. A gradual build-up is anticipated, proceeding from concept exploration towards Engineering, Manufacturing and Demonstration (EMD). A single-launch orbital demonstration is envisioned as part of this plan.

One cost we examine in this study is the cost of propellant resupply. The Space Dock in the operations concept represents a method to spread the cost of multiple missions over the price of one launch. Propellant must be launched to LEO using a conventional launch vehicle and the space dock enables use of its maximum payload capacity.

Table 5 shows launch costs to re-supply propellant. The table shows the best cost per 28.5-degree 8-ton mission is $13.3M, or $19.1M per 51.2-degree mission using Falcon Heavy. In comparison to Kutter et al [1] who supposed a profit at $5M per ton of propellant, the Falcon Heavy achieves $1.54M per ton.

Table 5, Mission Launch Costs

Vehicle	Price ($M)	Mass to LEO (kg)	Num 8-MT Missions (28.5)	Cost per mission ($M)	Num 8-MT Missions (51.2)	Cost per mission ($M)
Atlas V (401)	$109	9800	1.1	95.95	0.8	-
GSLV Mk2	$54	5000	0.6	-	0.4	-
Atlas V (411)	$115	12000	1.4	82.66	1.0	119.21
Atlas V (421)	$123	13000	1.5	81.61	1.0	117.69
Atlas V (431)	$130	15000	1.7	74.75	1.2	107.8
Atlas V (541)	$145	17000	2.0	73.57	1.4	106.1
Atlas V (551)	$153	18856	2.2	69.98	1.5	100.93
Ariane 5 ES	$166	21000	2.4	68.18	1.7	98.33
Soyuz ST	$48	7100	0.8	-	0.6	-
Proton M	$95	23000	2.7	35.63	1.8	51.38
Falcon 9	$61	22800	2.6	23.08	1.8	33.28
Falcon Heavy	$98	63800	7.4	13.25	5.1	19.11

To be competitive with GTO launch services, the value of the service must exceed the cost of the client LEO launch plus the cost of the reusable service. We subtract from the Ariane 5 ECA mission cost the price of a Falcon 9 LEO launch, indicating an equitable price of $159M. Falcon Heavy provides corroboration in its top price of $150M. A likely price for the mission is $150M per client.

If two payloads in the manifest are assumed, Falcon heavy theoretically launches propellant sufficient for 7.4 OTV missions per Falcon launch. Using the above pricing of $150M per payload, and assuming 6 PMKs can be stacked within the Falcon Heavy payload envelope, revenues can be 136 times launch costs.

$$6 * \$300/\$13.25 \cong 136$$

A design challenge is to develop a launch vehicle payloadconfiguration that maximizes the propellant mass per launch.

Our estimate of operating profit is $794M per year on $1500M in revenues, for a service operating 4 multiple-manifest missions per year and using Falcon Heavy for propellant resupply. To achieve this mission rate, a minimum fleet of 4 vehicles is required.

If realized, the envisioned reusable orbit transfer service is likely to meet both its business and technical objectives.

Appendix

A. Melbourne and Sauer Mass Optimization

Melbourne and Sauer perform analytical optimization of power plant mass ratios and final mass ratios [12] for maximum payload ratio. There are several assumptions and differences in formulation that need to be considered.

Eq. (1) is reformulated as,

$$a(t) = {2\eta\alpha}\Big/{(\mu_W I_{sp} g_0)}$$

Where:

a(t) = specific acceleration
η = Power efficiency of the propulsion system
α = Specific Power (kg/kW)
μ_W = mass the power plant
I_{sp} = specific impulse
g_0 = 9.81-m/s^2

Their consideration of maximum payload for minimum time trajectories, which is exactly the case of Edelbaum-Alfano trajectories, leads to minimizing the integral of $a(t)^2$,

$$\int_{t_0}^{t_f} a(t)^2 dt = {2\eta\mu_W}\Big/{\alpha}\left({1}\Big/{\mu_{bo}} - {1}\Big/{\mu_0}\right) \tag{4}$$

Where:

t_0 = initial time
t_f = time of arrival in final orbit
μ_{bo} = mass at t_f
Note that ${\eta\mu_W}\Big/{\alpha}$ is thrust power in kW

Melbourne and Sauer offer simple approximations for this optimization, for use in preliminary mission analysis. The optimum value for μ_W which maximizes the payload mass is,

$$\mu_W \cong \mu_{bo}(1 - \mu_{bo}) \tag{5}$$

$$\mu_{bo} \cong \left(1 - {\gamma}\Big/{\eta^{1/2}}\right) \tag{6}$$

$$\gamma^2 = \frac{\alpha}{2}\int_{t_0}^{t_f} a(t)^2\, dt = \eta\mu_W\left({1}\Big/{\mu_{bo}} - {1}\Big/{\mu_0}\right) \tag{7}$$

Using Eq. (4) through (7) we can identify configurations with near optimum μ_W. As discussed in the text of the report, configurations which are optimum for only the 4000-kg payload class are not considered since these do not support a multiple manifest.

In Table 6, the optimum μ_W is calculated starting with Eq. (7), the result is substituted into Eq. (6) giving optimum μ_{bo}, which is substituted in-turn into Eq. (5) yielding the value of optimum μ_W. The result of Eq. (5) is subtracted from the modeled power supply mass ratio and differences less than 0.03 are identified as the configurations closest to the optimum for the given payload.

Note that the 32x8061 configuration is the only configuration that is optimum through the range of 8000 to 12000-kg payload mass.

Two larger configurations, 64x6295 and 64x8061, are also assessed in Table 6 and found to be optimum for transport of much larger payloads, up to 36,000-kg.

Table 6, Optimized Power Supply Mass per Vehicle Configuration

Power (kW)	Ms	Mw	Mpl	Mbo	Mprop	M0	mu-w	Opt. mu-w	Criteria
32x4537W									
150.18	3090.41	2934.37	8000	14024.78	6234.20	20258.98	0.145	0.189	0.045
150.18	3090.41	2934.37	12000	18024.78	7705.60	25730.38	0.114	0.172	0.058
32x6295W									
206.44	3125.66	3962.43	8000	15088.09	7004.48	22092.57	0.179	0.205	0.026
206.44	3125.66	3962.43	12000	19088.09	8475.18	27563.27	0.144	0.189	0.045
32x8061W									
262.95	3179.71	5674.73	8000	16854.44	8283.38	25137.82	0.226	0.222	0.004
262.95	3179.71	5674.73	12000	20854.44	9754.22	30608.66	0.185	0.208	0.022
64x6295W									
407.88	5207.89	11047.87	16000	32255.76	15921.78	48177.54	0.229	0.223	0.006
407.88	5207.89	11047.87	24000	40255.76	18863.18	59118.94	0.187	0.208	0.021
407.88	5207.89	11047.87	36000	52255.76	23275.28	75531.04	0.146	0.190	0.044
64x8061W									
520.90	5297.19	15720.53	16000	37017.72	19390.56	56408.28	0.279	0.236	0.043
520.90	5297.19	15720.53	24000	45017.72	22332.10	67349.82	0.233	0.224	0.009
520.90	5297.19	15720.53	36000	57017.72	26744.20	83761.92	0.188	0.209	0.021

B. Mass Model

The mass properties of the vehicle used in this analysis are constructed from a bottom up estimate which is calculated for given number of thrusters, power requirements and payload mass. The mass budget is implemented in a worksheet that calculates the mass of structure, propulsion, thermal radiators and power plant based upon the number of Hall-Effect Thrusters, their specific impulse and vehicle layout based on required dimensions for solar array and thermal radiator clearance.

In as many cases as possible, the mass estimate is based upon actual manufacturer's data, for catalog products, in other cases the model resorts to analytical estimates such as found in SMAD Table 14-18 [23]. The SMAD criteria are used to estimate the mass of the Attitude Control, Command and Data Handling, and Telemetry, Tracking and Command subsystems.

Solar array mass is based upon the Spectrolab XJT Prime solar panels with 6-mil ceria coverslips supported by composite substrate, a density of 2.06 kg/m2 is used in the mass model plus 20%. Solar Array wings are each sized for EOL with 6 panels per wing. Power electronics is sized at 680 W/kg per AIAA 2009-4613. Power harness mass is estimated based on the calculated path length from solar array tip to mid propulsion bay using the mass properties of Mil-W-22759/3-1, with 1/1 cables and two cables per wing. Batteries are required for cathode standby power during eclipse and are sized based upon the SAFT Lithium ION cell at 80% depth of discharge using an estimate of 200W-hr per cathode.

Thermal panels are based upon panels available from the TMT company with a heat dissipation into -20-degC of 533 W/m^2. Structure is estimated as carbon composite tubing at 0.47 kg/m with a factor of 2.5 for Titanium fittings and mating mechanisms. Titanium bearing surfaces are cobalt-nickel coated or equivalent. Propellant mass is calculated based upon a 21% propellant mass fraction that is derived from the trajectory analysis.

Results of these calculations are reported in Table 6 above, and in Table 4, Vehicle Configuration.

C. Trajectory Simulations

To account for thrust variation due to Eclipse, GMAT simulations are performed for Epochs that span the four seasons, Winter Solstice, Vernal Equinox, Summer Solstice, and Autumnal Equinox in year 2020. The GMAT

Electric Propulsion model is renamed HET and set for Constant Thrust and Isp. The Isp, thrust, minimum power and maximum power is set on a case by case basis per Table 4 for each different configuration studied.

The Solar Power System Model Initial Max Power is set per Table 4 on a case-by-case basis. The Dual Cone shadow model is used with earth as a Shadow Body and the housekeeping power budget (Coefficient 1) is set to 0.5 kW.

Radiation degradation of the arrays is set to 1.7 percent per year based on Spectrolab data sheets for XTJ Prime Solar Cells which are advertised at 26.7% power End of Life for a 1E15 1MeV electron fluence [24]. The mass of these arrays is estimated based on a composite substrate, 5mil ceria doped coverslip and the panel density value provided by Spectrolab product literature.

The GMAT Spacecraft Epoch is set on a case-by-case basis to account for the four eclipse seasons in-orbit. The EarthMJ2000Eq coordinate system is used with a Keplerian state per Table 7.

Table 7, GMAT Spacecraft Model Parameters

Element	Value	Units
Epoch format	UTC Gregorian	
SMA	6878.136	km
Eccentricity	0.01	
Inclination	51.2 or 28.5	deg
RAAN	360	deg
Argument of Perigee	180	deg
True Anomaly	90	deg
Coefficient of Drag (Skylab)	4	
Coefficient of Refl. (default)	1.8	
Drag Area (Skylab minimum)	14.2	sq. m
SRP Area (default)	1	sq. m

A balance between propagator convergence and thrust direction computation was found using the Prince-Dormand78 integrator. The integrator is used with an initial step size of 30, a max step size of 3000, and an accuracy of 1e-007. A four by four JGM-2 gravity model and spherical Solar Radiation Pressure model is used.

The Wiesel-Alfano trajectory is implemented using the Eq. (3), the Edelbaum yaw control law. The optimization of the trajectory is achieved by solving the two-point boundary value problem represented by the Euler-Lagrange costates for a value of the inclination costate at the boundary. This results in a polynomial of complete elliptic integrals and their derivatives. Alfano's method involves finding the value of the costate by graphical means, solving the inverse of the Phi function and then substituting the resultant "control variable", a scale factor, into Eq.3 to derive maximum yaw angle for each orbit revolution.

Costates result from the solution of the Lagrangian partial differential equations using the method of undetermined multipliers to adjoin the constraint equations to the Hamiltonian. The costates are the functional solutions to the constraint equations.

We obtain the control law scale factor by using the Phi function to forward calculate all values of costate in a linear range of the control variable and orbit ratio. This calculation is performed to 7 places of accuracy and stored in a database table, with foreign key the orbit ratio. The database is then used to find the values of the control variable in the domain of the Phi function for the range of orbit ratio desired.

The results of this process are depicted in Figure 12.

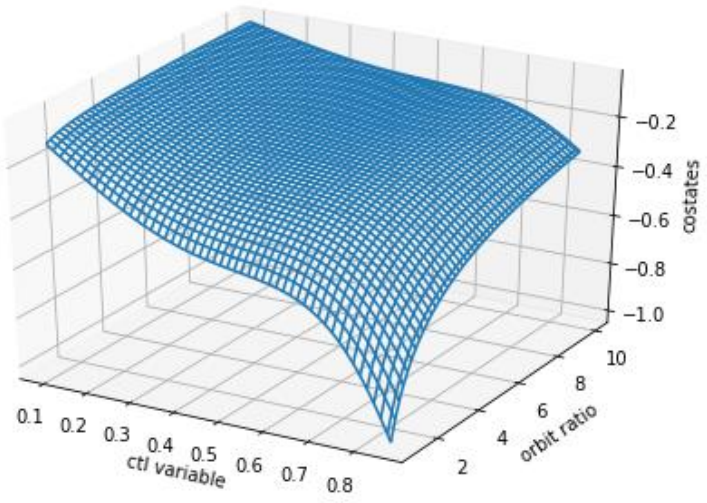

Figure 12, Plot of the Wiesel-Alfano Inclination Costate

Eclipse is a concern in the determination of time and fuel in this model. The method used to account for discontinuous thrust is informed by Kluever [22], wherein he divides the orbit period into intervals as follows.
Where:

$$t_{k+1} = t_k \frac{\Delta V_{k+1} - \Delta V_k}{\bar{A} w_k} \tag{9}$$

$\bar{A}$, the average thrust acceleration in interval k
w_k, a weight dependent on the size of the eclipse shadow arc

Kluever divides the orbit into adaptive time steps based on Eq. (9), this is basically dictating the propagator step times, which is impossible in GMAT without recoding the integrator; GMAT does not provide a means of programmatically enforcing a specific integrator step time. It is more expedient to simply let GMAT average the thrust in each integration interval.

As discussed in Kluever, there is very little eccentricity change due to yaw pitch control. Eclipse primarily affects the nodes and the argument of perigee (AOP). We nullify effect of the change in argument of perigee by using the Argument of Latitude in the control law, rather than True Anomaly as in Wiesel and Alfano. True Anomaly is technically undefined for a circular orbit.

The asymmetric thrust profile due to eclipse also causes a precession of the nodes. This is not important since the final orbit is circular. An inexpensive drift to the proper geosynchronous longitude corrects the error caused by nodal precession.

Another effect of eclipse is that the Wiesel-Alfano trajectory sometimes undershoots or overshoots the final inclination. This reliably occurs in transfers conducted during the summer and winter seasons whereas transfers at the equinoxes are unaffected. The effect is detectable in the arrived inclination which will be near 0.5 degrees if the transfer overshoots, or early arrival at inclination prior to the geosynchronous SMA being achieved. Given the accuracy setting of the Prince-Dormand integrator, the best inclination values achieved is 0.02 degrees of inclination. It is easy to adjust the costate value up or down slightly to achieve the 0.02 arrival inclination.

Lowering the costate value has the effect of performing a more aggressive inclination change, we find that an increase of 0.0025 in the costate value will correct the overshoot. We also adopted the non-optimal approach of resorting to tangential burns in the case of an undershoot, which simply raises the orbit radius to 42159-km once inclination is less than or equal to 0.02.

Acknowledgments

The author would like to recognize and thank the Busek Company, Specifically Dan Williams and Bruce Pote for review of this paper and James Szabo for providing updated technical specifications for the BHT-8000 Hall Effect Thruster.

This work has been created under the sponsorship of the American Institute for Research into Science and Technology.

References

[1] Kutter, Bernard F. United Launch Alliance, "AIAA 2016-5491, Cislunar-1000: Transportation supporting a self-sustaining Space Economy," in *AIAA SPACE Forum/SPACE 2016*, Long Beach, 2016.

[2] T. M. Perrin and J. G. Casler, "Architecture Study for a Fuel Depot Supplied From Lunar Resources," in *AIAA SPACE Forum, SPACE 2016*, Long Beach, CA, 2016.

[3] J. Fikes, J. T. Howell and M. Henley, "IAC-06-D3.3.08, In-Space Cryogenic Propellant Depot (ISCPD) Architecture Definitions and Systems Studies," in *57TH International Astronautical Congress*, Valenica, Spain, 2006.

[4] Arianspace, "Ariane 5 User's Manual, Issue 4," Arianspace, Evry, France, 2004.

[5] S. Clark, "Ariane 5 Goes on Test Run After Launching Two Satellites," *Spaceflight Now,* 5 October 2016.

[6] United Launch Alliance, "Atlas V Launch Services User's Guide," 2010.

[7] S. Clark, "India Tests Upgraded Engine Tech in Successful Communication Satellite Launch," *Spaceflight Now,* 29 March 2018.

[8] NASA Goddard Spaceflight Center, "GMAT Central," 22 Nov 2012. [Online]. Available: http://gmatcentral.org/. [Accessed 31 May 2018].

[9] The Times of India, "ISRO Successfully Launches Communication Satellite GSAT-6A," Times Now, 29 Mar 2018. [Online]. Available: https://timesofindia.indiatimes.com/videos/news/isro-successfully-launches-communication-satellite-gsat-6a/videoshow/63535170.cms. [Accessed 2 April 2018].

[10] S. C. Gupta, B. N. Suresh and K. Sivan, "Evolution of Indian Launch Vehicle Technologies," *Current Science,* vol. 93, no. 12, p. 1700, 2007.

[11] Lockheed Martin Corporation, "Form 10-K United States Security and Exchange Commission," USPO, Washington DC, 2017.

[12] W. G. Melbourne and C. G. Sauer Jr., "Payload Optimization for Power Limited Vehicles," in *Progress in Astronautics and Aeronautics, Volume 9: Electric Propulsion Development*, vol. 9, E. Stuhlinger, Ed., Berkely, CA, Elsevier, 1963, pp. 617-646.

[13] T. W. Kerslake and L. P. Gefert, "Solar Power System Analysis for Electric Propulsion Mission," NASA Glenn Research Center, Cleveland, OH, 1999.

[14] T. R. Sarver-Verhey, T. W. Kerslake and et-al, "Solar-Electric Propulsion Vehicle Design Study for Cargo Transfer to Earth-Moon L1," Glenn Research Center, NASA, Cleveland, OH, 2002.

[15] Viasat, Carlsbad, "Viasat and Boeing Proceeding with Full Construction on the First Two Viasat-3 Satellites," PRNewswire, 25 Sep 2017. [Online]. Available: https://www.viasat.com/news/viasat-and-boeing-proceeding-full-construction-first-two-viasat-3-satellites. [Accessed 28 Oct 2017].

[16] NASA Glenn Research Center, "FS-2000-11-006-GRC, Powering the Future," NASA, Cleveland, OH, 2000.

[17] J. Szabo, B. Pote, L. Byrne and et-al, "Eight Kilowatt Hall Thruster System Characterization," in *33rd International Electric Propulsion Conference*, Washington D.C., 2013.

[18] D. Williams, Interviewee, *Director of Business Development, Busek Company.* [Interview]. 09 June 2018.

[19] D. A. Vallado, Fundamentals of Astrodynamics and Applications, Table 6-2, Hawthorne, CA: Microcosm, 2013, p. 341.

[20] W. Wiesel and S. Alfano, "Optimal Many-Revolution Orbit Transfer," *Journal of Guidance and Control,* vol. 8, no. 1, pp. 155-157, 1985.

[21] A. J. Kechichian, "Low-Thrust Inclination Control in Presence of Earth Shadow," *Journal of Spacecraft and Rockets*, vol. 35, no. 4, pp. 526-532, 1997.

[22] C. A. Kluever, "Using Edelbaum's Method to Compute Low-Thrust Transfers with Earth-Shadow Eclipse.," *Journal of Guidance and Control*, vol. 34, no. 1, pp. 300-303, 2011.

[23] J. R. Wertz, D. F. Everett and J. J. Puschell, Space Mission Engineering: The New SMAD, Hawthorne, California: Microcosm Press, 2011.

[24] Spectrolab, "Spectrolab - A Boeing Company," 2009. [Online]. Available: http://www.spectrolab.com/DataSheets/cells/XTJ_Prime_Data_Sheet_7-28-2016.pdf. [Accessed 28 October 2017].

[25] Spaceflight Now, "Launch Log," 2018. [Online]. Available: https:spaceflightnow.com/tracking/launchlog.html. [Accessed 30 May 2018].

[26] SpaceX, "Falcon 9 Launch Vehicle Payload User's Guide," 2015.

[27] SpaceX, "Falcon-Heavy," SpaceX, 2017. [Online]. Available: http://www.spacex.com/falcon-heavy. [Accessed 30 May 2018].

[28] United Launch Alliance, "Rocket Builder," 30 May 2018. [Online]. Available: https://www.rocketbuilder.com/start. [Accessed 12 03 2018].

[29] Wade, "Encyclopedia Astronautica," Encyclopedia Astronautica, 2017. [Online]. Available: www.astronautix.com. [Accessed 25 March 2018].

[30] D. A. Vallado, Fundamentals of Astrodynamcis and Applications, 4th ed., Hawthorne, CA: Microcosm Press, 2013, pp. 381 - 388.

[31] Spectrolab, "Space Solar Panels Brochure," 2010. [Online]. Available: www.spectrolab.com. [Accessed 12 November 2017].